An iterative data-driven learning algorithm for calibration of the internal model in advanced wind turbine controllers

Mulders, Sebastiaan P.; Liu, Yichao; Spagnolo, Fabio; Christensen, P.B.; van Wingerden, Jan Willem

DOI
10.1016/j.ifacol.2023.10.1035

Publication date
2023

Document Version
Final published version

Published in
IFAC-PapersOnLine

Available online at www.sciencedirect.com

ScienceDirect

IFAC PapersOnline CONFERENCE PAPER ARCHIVE

IFAC PapersOnLine 56-2 (2023) 8406–8413

An iterative data-driven learning algorithm for calibration of the internal model in advanced wind turbine controllers ⋆

Sebastiaan P. Mulders * **Yichao Liu** * **Fabio Spagnolo** †
Poul B. Christensen † **Jan-Willem van Wingerden** *

* *Delft University of Technology, Delft Center for Systems and Control, Mekelweg 2, 2628 CD Delft, The Netherlands* {*S.P.Mulders, J.W.vanWingerden*}*@tudelft.nl.*

† *Vestas Wind Systems A/S, Hedeager 42, 8200 Aarhus N, Denmark.*

Abstract: Modern industrial wind turbine controllers for partial-load region control are becoming increasingly complex by progressively relying on modeled aerodynamic characteristics. These advanced turbine controllers generally consist of a combined wind speed estimator and tracking controller, allowing for a granular trade-off between energy capture maximization and (fatigue) load minimization. Because of the limited measurements available to the controller, the control scheme's internal model quality is of utmost importance in satisfying performance and stability requirements. Therefore, the calibration thereof is of particular interest. To date, little work has been performed on the direct calibration of the model information. This work proposes a data-driven iterative learning algorithm for calibrating the internal physical model parameters. The learning algorithm uses generally available closed-loop turbine measurements, complemented with an external measurement of the rotor effective wind speed (REWS), and is thereby largely nondisruptive. The algorithm is based on steady-state assumptions and performs iterative batch-wise updates of the internal control model toward convergence. As the algorithm corrects at the actual turbine operating point, short-term relocations of the turbine's operating point can be used to calibrate in a broader operational domain. Results show outstanding learning capabilities for an aerodynamically degraded wind turbine under realistic turbulent wind conditions. Moreover, a sensitivity study is performed to expose the algorithm's susceptibility to measurement errors, algorithm tuning, and the size of the data set.

Keywords: Learning for control, Data-driven control, Control of renewable energy resources, Nonlinear adaptive control, Nonlinear observers

1. INTRODUCTION

Wind energy plays an increasingly pivotal role in the ambition to meet the Paris Agreement target of limiting global warming to 1.5 °C. In July 2021, the European Commission proposed a new 2030 climate target to increase the share of renewable energy sources to at least 40 %. With a record of 837 GW of global installed wind in 2021 (Global Wind Energy Council, 2022), the capacity is expected to further increase by 116 GW between 2022 – 2026 (Komusanac et al., 2022). In attaining these strong ambitions, the most cost-effective and economically viable solution for wind energy is to increase the turbine-rated power outputs, which consequentially demands even larger turbine sizes (Burton et al., 2001). Advanced and highly optimized wind turbine controllers are essential in accelerating this development in empowering wind power's next era of growth (Veers et al., 2019).

The industry's current partial-load region power control practice combines an advanced wind speed estimator and tip-speed ratio (WSE-TSR) tracking control scheme. In contrast to the classical $K\omega^2$ torque control strategy (Jonkman et al., 2009), the WSE-TSR tracking scheme unleashes the potential to improve power extraction performance. It provides means for a more granular trade-off between loads and energy capture (Bossanyi, 2000; Abbas et al., 2022). In this scheme, the rotor-effective wind speed (REWS) estimate (Soltani et al., 2013) obtained from the wind speed estimator is used to compute an error signal to the TSR tracking controller.

In a study of Brandetti et al. (2022), the WSE-TSR tracking scheme was found to be inherently ill-conditioned. An in-depth frequency-domain analysis illustrates that uncertainties in the internal control model lead to biased effective wind speed estimates. As a result of the ill-conditioning, the operating condition of the real-world wind turbine deviates from the reference set point in the presence of model uncertainty, potentially resulting in suboptimal performance and stability issues.

The accuracy of the wind speed estimate is highly dependent on the internal model's resemblance to the wind turbine's actual aerodynamic properties. Often, these modeled parameters diverge initially from the actual aerody-

⋆ This research was conducted in cooperation with Vestas Wind Systems A/S.

10.1016/j.ifacol.2023.10.1035

namic rotor characteristics and vary further over time due to, e.g., blade erosion and ice/dirt/bug build-up (Fingersh and Carlin, 1999; Johnson et al., 2006). Therefore, developing methods for calibrating the internal control model is of particular interest to sustain control performance.

Several direct and indirect learning schemes have been developed for optimizing partial-load region power control. For example, for the classical $K\omega^2$ control scheme, a direct adaptive torque control law targeting the optimization of the generator torque gain K, based on a combined perturb and observe (P&O) and maximum power point tracking (MPPT) strategy, was proposed and evaluated for stability by Johnson et al. (2004). A related model-free extremum seeking control (ESC) approach based on logarithmic power feedback was introduced by Rotea (2017).

The above-presented researches mainly focus on the direct optimization of the controller. In contrast, limited studies investigated the calibration of physical turbine properties represented by, e.g., the rotor power coefficient characteristics. For example, Lio et al. (2021) suggested the reconstruction of the power coefficient mapping with Gaussian process regression based on standard real-time turbine measurements. Another study introduced an online method to estimate the power coefficient by measuring the wind speed, generator voltage, and electrical current (De Kooning et al., 2013). The authors of the current work recently established an excitation-based learning scheme that does not depend on wind speed measurements (Mulders et al., 2023a).

In contrast to the abovementioned work, this paper proposes an excitation-free learning algorithm, taking advantage of the structure and information in advanced wind turbine controllers. The proposed learning algorithm assumes that the rotor effective wind speed (REWS) is measurable. In practice, such wind speed information can be obtained from the turbine anemometer or accurate light detection and ranging (LIDAR) measurement device used only during a short-term calibration campaign. The algorithm is unique in learning an aerodynamic degradation function iteratively by updating the internal model information toward convergence. Furthermore, the algorithm is efficient by taking advantage of the uncertainty in the internal model to learn in a broader operational domain.

In summary, the following contributions are presented in this paper:

(1) Demonstrating that with the knowledge of specific measured quantities, a degradation function can be learned in a purely data-driven and iterative way by periodically updating the internal control model.
(2) Showing that the effects of ill-conditioning under model uncertainties in the control system can be exploited by learning and calibrating the internal model at the actual operating point.
(3) Presenting the results of a complete learning cycle based on high-fidelity simulations.
(4) Performing sensitivity analyses considering wind speed measurement offsets and algorithm tuning.
(5) Providing a publicly available software implementation of the learning algorithm (Mulders et al., 2023b).

The remainder of this paper is structured as follows. First, Section 2 presents the methodological theory and derivations of the WSE-TSR tracking scheme that is considered in this paper. Next, Section 3 provides a derivation of the critical analytical results the algorithm is based upon. Subsequently, Section 4 provides the implementational details of the algorithm and discusses its working principles by an illustrative example showing complete-cycle learning results. Section 5 provides a sensitivity analysis of the learning performance considering measurement errors, algorithm tuning, and data set size. Finally, conclusions are drawn in Section 6.

PREREQUISITES

Throughout the paper, vectors, and matrices are denoted in bold font, either lowercase ($\mathbf{x}$) or uppercase ($\mathbf{X}$) depending on the represented quantity. Functions of values indicating the modeled or intended optimal parameters are presented with $(\cdot)^\diamond$, whereas estimated quantities and uncertain modeled information are indicated by $\hat{(\cdot)}$. Values corresponding to a specific operating point are denoted by $\bar{(\cdot)}$, and the time derivative is indicated by $\dot{(\cdot)}$.

This study is based on the following assumptions:

Assumption 1. The turbine is assumed to only operate in the partial-load region subject to generator power control at a constant (fine-)pitch angle. Therefore, the power coefficient information is only taken as a function of the tip-speed ratio.

Assumption 2. Among all the modeled parameters in the WSE-TSR tracking scheme, only the power-coefficient information is assumed to be uncertain.

Assumption 3. An element-wise function multiplication induces power coefficient uncertainty for the entire domain of the power-coefficient array.

Assumption 4. The rotor-effective wind speed is accurately measured and is only used by the learning algorithm during a calibration campaign.

Assumption 5. The drivetrain's efficiency is assumed to be lossless, and no generator dynamics are considered. Thereby, the power control set point is equal to the measured generator power and in steady-state equal to the rotor power.

2. METHODOLOGY

This section provides a derivation of the considered advanced wind turbine control scheme, being the WSE-TSR tracking controller. After its formal definition, the way of incorporating model uncertainties in the controller framework is described.

2.1 Wind turbine control scheme

In modern wind turbines, the tip-speed ratio tracking controller is usually combined with a rotor-effective wind speed estimator. This partial-load control scheme aims to regulate the rotor at desired aerodynamic operating conditions, thereby simultaneously controlling the generator power. A block diagram of the control scheme considered in this paper is presented in Fig. 1 and is referred to as the

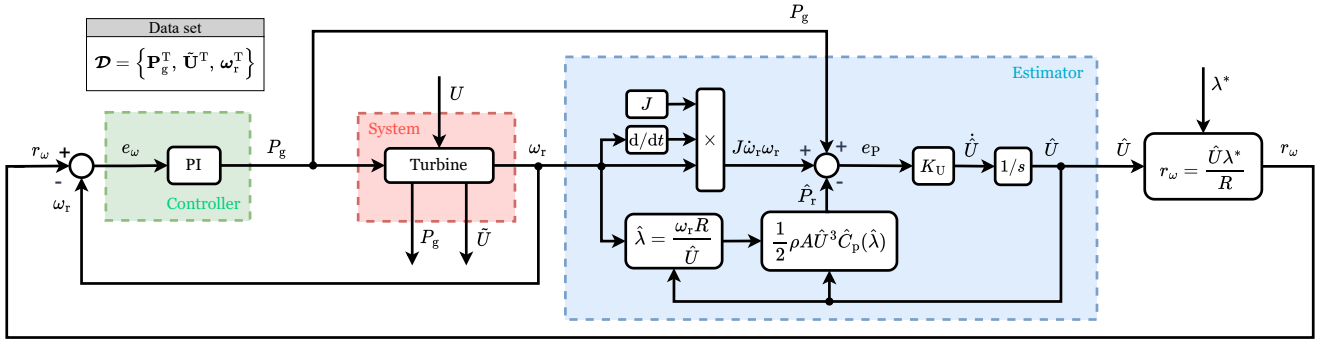

Fig. 1. Block diagram of the partial-load wind turbine controller. The red box contains the wind turbine system, with as input the generator power set point P_g, and as outputs the measured rotor speed ω_r, the measured and filtered rotor-effective wind speed $\tilde{U}$, and measured generator power P_g. The turbine is subject to an actual REWS disturbance U. The wind speed estimator is indicated in blue and relies on the system in- and output and a nonlinear internal model of the wind turbine to estimate the rotor-effective wind speed $\hat{U}$. This estimate is used to compute the rotor speed set point r_ω resulting in the error e_ω by subtracting ω_r. The error signal is provided to the PI controller indicated in green. The controller provides the generator power set point P_g. During nominal closed-loop operation, a data set $\mathcal{D}$ from the turbine outputs is collected for the learning algorithm.

WSE-TSR tracking scheme. Only the main results of the distinct elements in the scheme are given in this work; the reader will be referred to other works for more extensive derivations.

The wind turbine is represented as a first-order system

$$J\dot{\omega}_r(t)\omega_r(t) = P_r(t) - P_g(t)\,, \tag{1}$$

in which $J \in \mathbb{R}$ denotes the effective rotor inertia at the low-speed shaft (LSS), $\omega_r \in \mathbb{R}$ the rotor speed, and $P_r \in \mathbb{R}$ and $P_g \in \mathbb{R}$ the respective aerodynamic power and generator power set point, the latter of which is assumed to be directly related to the measured generator power (Assumption 5). The time indication t is omitted from this point unless its inclusion improves clarity. The aerodynamic power is given by

$$P_r \triangleq \frac{1}{2}\rho A U^3 C_P(\lambda)\,, \tag{2}$$

where $\rho \in \mathbb{R}$ is the fluid (air) density, $A \in \mathbb{R}$ the rotor swept area, $U \in \mathbb{R}$ the rotor effective wind speed, and $C_P : \mathbb{R} \to \mathbb{R}$ the rotor power coefficient mapping as a function of the dimensionless tip-speed ratio

$$\lambda = \omega_r R/U\,, \tag{3}$$

with R being the rotor radius (Assumption 1).

The employed wind speed estimator is a dynamic variant of the commonly applied power (or torque) balance equation (Bossanyi, 2000), which shows a high degree of similarity with the immersion and invariance (I&I) estimator (Ortega et al., 2013; Liu et al., 2022). It is given by

$$\dot{\hat{U}} = K_U e_P = K_U\left(P_g - \hat{P}_r + J\dot{\omega}_r\omega_r\right)\,, \tag{4}$$

where K_U is the estimator gain, and the estimated aerodynamic rotor power is defined as

$$\hat{P}_r = \frac{1}{2}\rho A\hat{U}^3\hat{C}_P(\hat{\lambda})\,, \tag{5}$$

with $\hat{\lambda} = \omega_r R/\hat{U}$.

The tip-speed ratio tracking controller is implemented as a proportional-integral (PI) controller

$$\dot{P}_g = K_p\dot{e}_\omega + K_i e_\omega\,, \tag{6}$$

where the error $e_\omega = r_\omega - \omega_r$ is the difference between the respective rotor speed and the time-varying rotor speed set point $r_\omega(t)$, obtained using (3) with the desired tip-speed ratio λ^* and the estimated wind speed $\hat{U}$.

2.2 Internal model uncertainty

In this section, the derivation of the considered wind turbine system is complemented by a definition of internal model uncertainty. The uncertainty is the quantitative degree of dissimilarity between the actual and modeled turbine aerodynamic properties in a considered turbine operating range.

Under Assumption 2 and 3, this paper considers the model uncertainty as a multiplicative degradation function acting on the ideal (modeled) aerodynamic rotor properties:

$$C_P(\lambda) \triangleq \Gamma(\lambda)C_P^\diamond(\lambda)\,. \tag{7}$$

Note that the degradation function $\Gamma(\lambda)$ is unknown in real-world scenarios.

Similarly, the power coefficient data included in and used for the overall control system is obtained by multiplication of the estimated degradation function with the ideal aerodynamic rotor properties:

$$\hat{C}_P(\hat{\lambda}) \triangleq \hat{\Gamma}(\hat{\lambda})C_P^\diamond(\hat{\lambda})\,. \tag{8}$$

Furthermore, by equating the steady-state result of aerodynamic rotor power and its estimate, i.e., $P_r = \hat{P}_r$, respectively defined by (2) and (5), and substituting the uncertainty expressions (7) and (8), one obtains

$$\hat{U}^3 = U^3\frac{C_P(\lambda)}{\hat{C}_P(\hat{\lambda})} = U^3\frac{\Gamma(\lambda)}{\hat{\Gamma}(\hat{\lambda})}\frac{C_P^\diamond(\lambda)}{C_P^\diamond(\hat{\lambda})}\,. \tag{9}$$

As shown, an accurate estimate of the actual REWS can only be made when $C_P(\lambda) = \hat{C}_P(\hat{\lambda})$. In the proposed uncertainty definition framework, this consequently means that a consistent estimate of Γ by $\hat{\Gamma}$ is required. The uncertainty calibration problem tackled in this paper is thereby formulated as follows:

Problem statement: Consider a wind turbine (1) controlled by the tracking scheme in (4)–(6) that is subject to aerodynamic degradation in (7). Find a consistent estimate of Γ, such that

$$\left|\Gamma(\lambda) - \hat{\Gamma}(\hat{\lambda})\right| < \epsilon \; \forall \; (\lambda = \hat{\lambda}) \subset \Lambda \,,$$

with Λ being the complete operating range of the turbine, and ϵ a predetermined threshold.

3. THE LEARNING ALGORITHM

Following Assumption 4 on the availability of the REWS, the development of a learning scheme seems straightforward. However, as will be outlined and illustrated in the current and subsequent sections, the proposed learning algorithm is intriguing by its elegance. The algorithm is thereby:

- Concise in terms of analytical derivation and straightforward in its implementation.
- Excitation-free and nondisruptive by only using measurements obtained under closed-loop operation.
- Batchwise iterative by a data-collection, computation, and calibration steps towards convergence.
- Learning the aerodynamic characteristics at the actual turbine operating point.
- Able to exploit internal model uncertainty and the phenomenon of ill-conditioning to learn in a broader domain around the commanded control reference.

The reader is referred to Brandetti et al. (2022) for a detailed description of the ill-conditioning present in state-of-the-art wind turbine controllers. Furthermore, under nominal closed-loop operation of the wind turbine according to the control scheme presented in Section 2, a data set is collected consisting of the following measured quantities:

$$\boldsymbol{\mathcal{D}} = \left(\mathbf{P}_\mathrm{g}^\mathrm{T},\; \tilde{\mathbf{U}}^\mathrm{T},\; \boldsymbol{\omega}_\mathrm{r}^\mathrm{T}\right) \in \mathbb{R}^{\mathrm{N}\times 3} \,, \tag{10}$$

where $\mathbf{P}_\mathrm{g} \in \mathbb{R}^{1\times \mathrm{N}}$ is a vector of P_g, $\tilde{\mathbf{U}} \in \mathbb{R}^{1\times \mathrm{N}}$ a vector of the measured and filtered REWS signal $\tilde{U}$, and $\boldsymbol{\omega}_\mathrm{r} \in \mathbb{R}^{1\times \mathrm{N}}$ a vector of ω_r. Furthermore, N is the amount of collected data samples of all the before-mentioned quantities.

The remainder of this section provides the fundamental analytical derivation, and results for the synthesis of the proposed data-driven learning algorithm in the subsequent section.

3.1 Analytical derivation

Consider the wind turbine operating under steady-state conditions ($\dot{\omega}_\mathrm{r} = 0$). Then, under Assumption 5, and in closed-loop operation of the wind turbine, the rotor, and measured generator power as in (2) is equal to the estimated aerodynamic rotor power represented by (5), such that:

$$P_\mathrm{g} = \hat{P}_\mathrm{r} \quad \rightarrow \quad K C_\mathrm{P}(\lambda) U^3 = K \hat{C}_\mathrm{P}(\hat{\lambda}) \hat{U}^3 \,, \tag{11}$$

with $K = \rho A/2$. Now, the estimated degradation function of (8) is explicitly represented with the presumption that $\Gamma(\lambda) \neq \hat{\Gamma}(\hat{\lambda}) \, \forall \, (\lambda = \hat{\lambda})$. Furthermore, the right-hand side wind speed and tip-speed ratio estimates are replaced with the filtered measurement-based quantities. The latter alteration leads to the critical observation and key ingredient for the proposed learning scheme that the previously defined equality becomes a steady-state inequality

$$P_\mathrm{g} \neq \hat{P}_\mathrm{r} \quad \rightarrow \quad K C_\mathrm{P}(\lambda) U^3 \neq K \hat{\Gamma}(\tilde{\lambda}) C_\mathrm{P}^{\diamond}(\tilde{\lambda}) \tilde{U}^3 \,, \tag{12}$$

with $\tilde{\lambda} = \omega_\mathrm{r} R/\tilde{U}$. The inequality is induced by the inconsistency of the modeled internal power coefficient information and the lack of the WSE-TSR scheme's balancing mechanism by introducing the external wind speed measurement. Appendix A explains this balancing mechanism more elaborately.

The measured generator power replaces the equation's left-hand side. Also, at the right-hand side, because now the measured wind speed is used, the modeled power coefficient information should be corrected locally by $\hat{\Gamma}$ at the actual average TSR operating point, such that:

$$P_\mathrm{g} \neq \hat{\Gamma}(\bar{\lambda}) \left(K C_\mathrm{P}^{\diamond}(\tilde{\lambda}) \tilde{U}^3 \right) , \tag{13}$$

and the actual average turbine operating point is approximated as

$$\bar{\lambda} \approx \frac{1}{N} \sum_{k=1}^{N} \tilde{\boldsymbol{\lambda}}(k) \,. \tag{14}$$

Naturally, this relationship only holds under steady-state conditions or when N is large enough to average out dynamic effects.

Finally, as all quantities in (13) are either known or measured except for $\hat{\Gamma}(\bar{\lambda})$, and by replacing the scalar variables with the measured vector quantities from $\boldsymbol{\mathcal{D}}$, the estimated degradation function is calibrated at $\bar{\lambda}$, by solving as follows

$$\hat{\Gamma}(\bar{\lambda}) = \boldsymbol{P}_\mathrm{g} \left(K C_\mathrm{P}^{\diamond}(\tilde{\boldsymbol{\lambda}}) \tilde{\boldsymbol{U}}^3 \right)^\dagger , \tag{15}$$

with $(\cdot)^\dagger$ representing the pseudoinverse.

4. IMPLEMENTATION AND RESULTS

This section synthesizes the proposed learning algorithm by exploiting the fundamental mathematics provided in Section 3. First, the implementational details are given, after which a complete learning cycle is presented by Fig. 2, wherein the degradation function for a specific aerodynamic degradation scenario is estimated.

4.1 Implementation details

This section provides further details for the effectuation of the learning algorithm. The considered wind turbine is taken as a first-order nonlinear model according to (1) and following the definition of the NREL 5-MW reference turbine (Jonkman et al., 2009). The simulation sampling time is $T_\mathrm{s} = 0.01$ s. Data is collected for 1500 s, of which the first 200 s are discarded to exclude transient effects, resulting in $N = 130,000$ data samples per measured signal. A realistic turbulent wind field is used with a mean speed of 7 m/s, following the IEC normal turbulence model (NTM) and class A turbulence characteristics (IEC, 2019).

The turbine's nominal power coefficient characteristics are assumed to be aerodynamically degraded according to

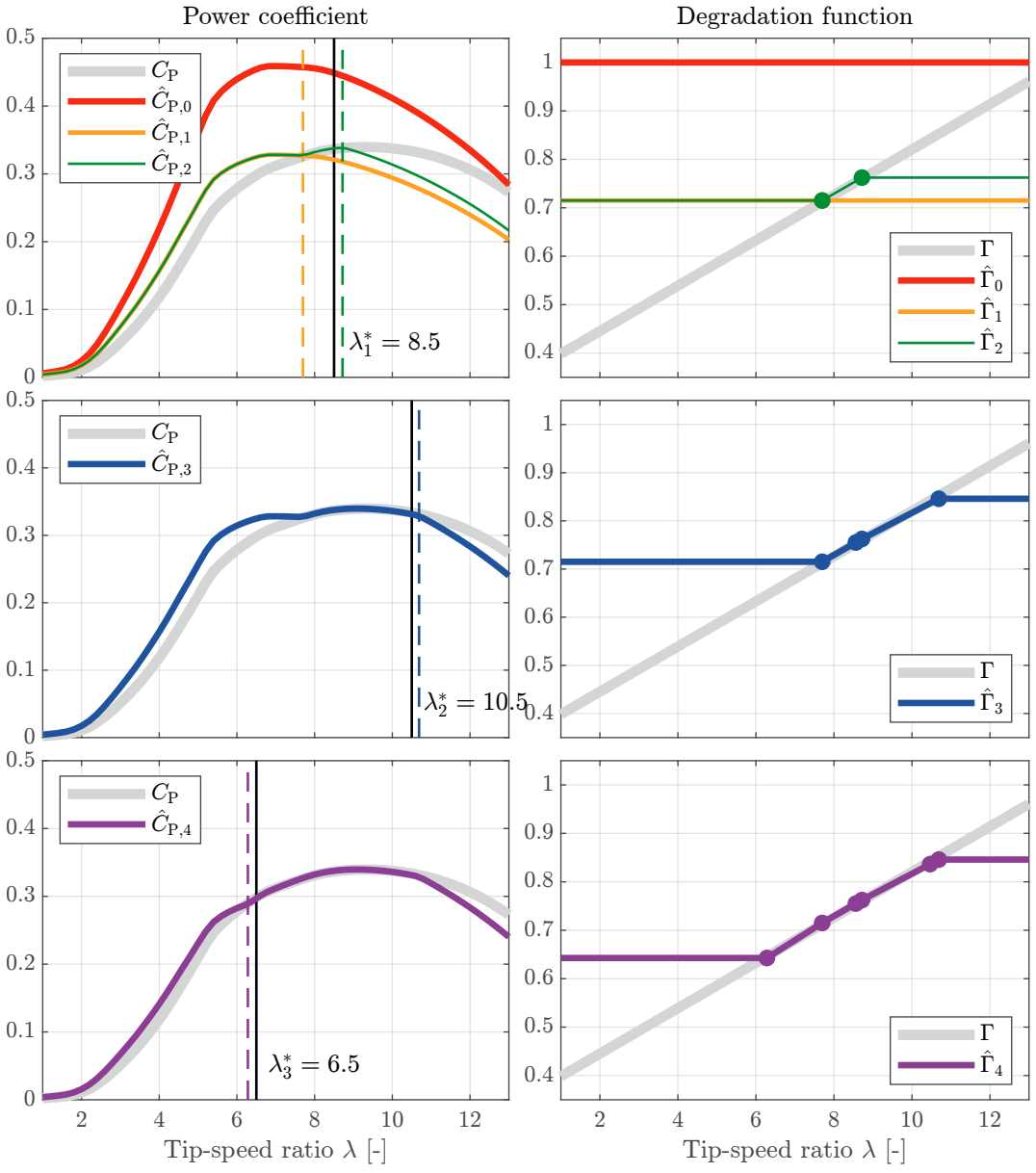

Fig. 2. A complete learning cycle of the proposed learning algorithm in different stages of the learning process. The left plots visualize the actual and estimated power coefficient trajectories, whereas the right plots show the corresponding learned degradation functions. All the figures include the actual power coefficient information C_P and related degradation function Γ and serve as a reference to the corresponding and subsequent estimated representations $\hat{C}_{P,i} = \hat{\Gamma}_i C_P^\diamond$. For this exemplary case, Γ is taken as a linear affine function as defined in (16).

First row: The estimated degradation function is initialized as $\hat{\Gamma}_0 = 1$, and the tip-speed ratio set point is set to $\lambda_1^* = 8.5$. After data collection of $\boldsymbol{\mathcal{D}}_1$, a single corrective calibration data point $(\cdot)$ is obtained and taken for the entire domain of $\hat{\Gamma}_1$. Next, by implementing $\hat{C}_{P,1}$ in the wind speed estimator and by repeating the same procedure, $\hat{\Gamma}_2$ is obtained. Again, after following the same procedure of updating, data-collection, and calibration, the algorithm converged for the region of λ_1^*. Note that the algorithm corrects at the actual operational tip-speed ratio of the wind turbine indicated by the vertical dashed lines. Furthermore, the iterative process illustrates the ability of the algorithm to exploit model uncertainty to learn and converge in the neighborhood of the TSR set point.

Second row: The turbine tip-speed ratio set point is (temporarily) relocated to λ_2^*. This is done to learn in a broader domain and because the algorithm can only learn at the actual operating point of the turbine. Again, the same data collection, computation, and implementation procedure of the updated power coefficient information is followed until convergence.

Third row: The last TSR set point relocation to λ_3^* and this calibration iteration represents the completion of the learning process. The final estimated degradation function $\hat{\Gamma}_4$ accurately reflects the actual turbine power coefficient properties throughout the explored domain.

the following (rather artificial) linear affine degradation function

$$\Gamma(\lambda) = \frac{3}{64}\lambda + 0.35\,, \tag{16}$$

as represented in Fig. 2 and is to be estimated by the learning algorithm.

The proposed learning algorithm relies on the availability of the data set $\boldsymbol{\mathcal{D}}_i$ throughout the consequent iterations i in the complete learning cycle. As seen in (10) and Assumption 4, a measured REWS signal is assumed to be available. For the considered case, the raw REWS signal U is filtered by an exponential filter

$$\tilde{U}(k) = \alpha\tilde{U}(k-1) + (1-\alpha)U(k)\,, \tag{17}$$

with the smoothing constant defined as $\alpha \triangleq \exp(T_s/\tau)$, and the filter time constant τ set to be 50 s.

4.2 Illustration of a complete learning cycle

This section describes the working principles of the proposed learning algorithm through full learning cycle results. Fig. 2 illustrates a complete learning cycle example with a detailed descriptive caption. This section complements the caption with further explanatory notes.

In the following, the index i indicates episodes of data collection and subsequent calibration, whereas j represents the instances when the tip-speed ratio set point is relocated for expanding the learning domain. The learning process is initiated in the first row of Fig. 2 by the collection $\boldsymbol{\mathcal{D}}_1$ in closed-loop operation of the turbine at the tip-speed ratio set point $\lambda^*_{j=1} = 8.5$. With $\boldsymbol{\mathcal{D}}_1$ at hand, $\bar{\boldsymbol{\lambda}}$ is computed offline and (15) is used to shape the estimated degradation function at $\bar{\lambda}_{i=1}$.

Due to the ill-conditioning problem in the considered partial load wind turbine control schemes (Brandetti et al., 2022), and as summarized in Appendix A, the presence of model uncertainty in the control scheme results in the commanded tip-speed ratio set point not being equal to the actual averaged TSR operating point. Therefore, after updating the internal power coefficient information in the WSE-TSR tracking scheme, another iteration $i = 2$ following the same procedure at an equal TSR set point is initiated. This learning routine is repeated until the following convergence criterion is met:

$$\left|\frac{\lambda^*_j - \bar{\lambda}_i}{\lambda^*_j}\right| < \epsilon\,, \tag{18}$$

with ϵ being a user-defined convergence constant.

Whenever the convergence criterion is satisfied, the TSR set point is relocated towards $\lambda^*_2 = 10.5$ as illustrated in the second row of Fig. 2. This set point alteration is performed such that the internal power coefficient can be reshaped in a broader operating region of the turbine. This lies in the fact that the learning algorithm can only learn at points where the turbine actually operates. The same procedure of iterative closed-loop data collection, calibration, and updating of the internal model is followed until convergence according to (18).

In the third row of Fig. 2, the procedure is executed for a final set point relocation $\lambda^*_3 = 6.5$. The result shows that $\hat{\Gamma}(\hat{\lambda})$ can be learned in a broad operating domain where actual turbine operation is feasible.

5. SENSITIVITY ANALYSIS

This section presents a sensitivity analysis of the learning performance of the proposed algorithm. The cases considered entail a bias in the filtered REWS measurement, the tuning of the wind speed filter time constant, and the data set iteration batch size.

For the studies in this section, the end-result distributions from complete learning cycles are completed for 10 wind realizations. These realizations represent equal wind properties and natural turbulence characteristics (NTM, class A). For comparison purposes, both the nominal and degraded function profiles are exhibited in all the results.

5.1 Rotor-effective wind speed bias

The REWS measurement, calculation, and filtering might introduce a static bias to the actual REWS value. Therefore, this section considers static offsets in the measurement of the REWS and analyses the effect on the algorithm results. Fig. 3 presents the complete learning cycle end-results for the set of wind speed offsets $\Delta U = \{-0.5, -0.25, 0, 0.25, 0.5\}$ m/s.

It is immediately apparent that a relatively small systematic measurement offset results in a substantial bias in the acquired estimated degradation function to the actual function. With (15) in mind, it is evident that the wind speed is taken cubically in the computation. As a result, a minor systemic deviation in the REWS value results in an exponentially increasing bias of the computed degradation factor. Furthermore, the 1σ uncertainty distribution is invariant for all considered cases.

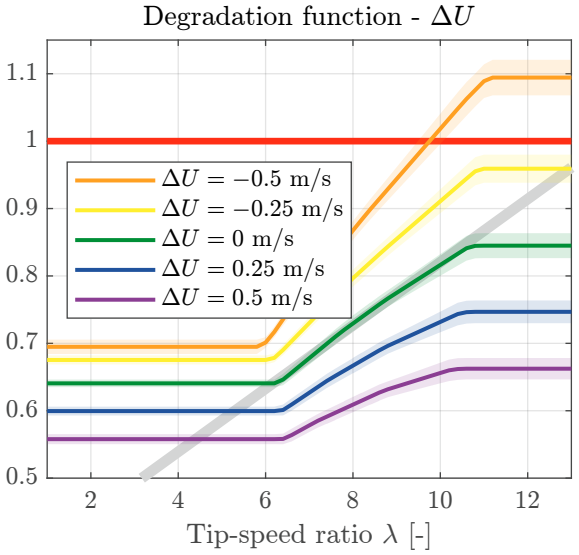

Fig. 3. Algorithm performance in learning the estimated degradation function for biased REWS measurements. While the obtained distribution (shaded) for all cases is negligible, the algorithm is susceptible to systematic wind speed measurement offsets.

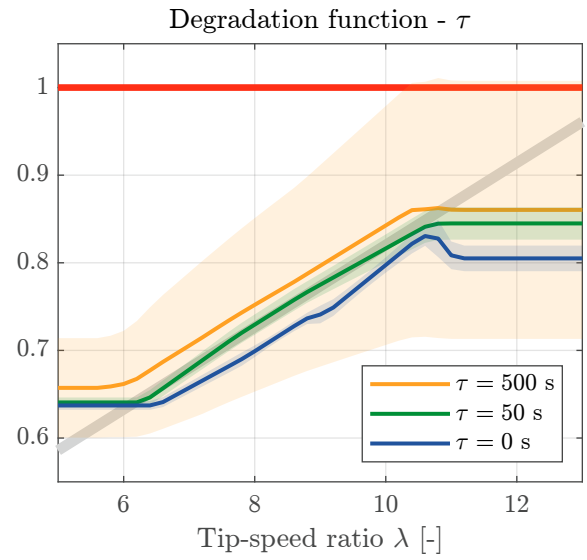

Fig. 4. Varying the wind speed filter time constant to evaluate its effect on the learning performance of the estimated degradation function. It is striking to observe that a perfect (unfiltered, $\tau = 0$ s) REWS measurement underperforms in terms of the estimated degradation function accuracy to the case when $\tau = 50$ s. For the severe-filtering case $\tau = 500$ s, the end-result distribution increases.

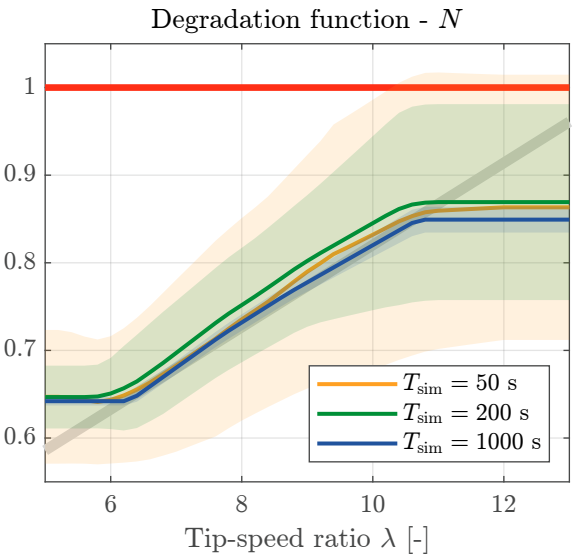

Fig. 5. Varying the data batch size in each learning iteration and its effect on the learning accuracy of the estimated degradation function. As expected, the variance over the learned degradation function decreases as data points increase. This effect is also caused by the derived algorithm being based on steady-state assumptions, such that the data set needs to be large enough to average out dynamic effects.

5.2 Filter time constant

Wind speed measurement devices may have ranging characteristics in terms of measurement bandwidth. Therefore, to mimic this behavior, this section presents a study varying the time constant τ defining the intensity of the exponential wind speed filter in (17). Fig. 4 presents the results for the following of filter time constants $\tau = \{0,\ 50,\ 500\}$ s.

The case for $\tau = 0$ s represents a perfect REWS measurement, whereas the two other cases of $\tau = 50$ s and $\tau = 500$ s, respectively, represent a realistic and severe filtering level. Remarkably, the end-result distribution for the realistic wind speed filtering case outperforms the unfiltered scenario. A plausible explanation is that the generator power signal includes the inertial response of the turbine drivetrain and rotor. Directly imposing an unfiltered REWS signal might result in incoherence between both, advocating for a filter (time-constant) that mimics the turbine response to wind variations. For severe filtering levels, the distribution over end results shows a high degree of variance. It is thus speculated that optimal filtering exists in attaining the most accurate representation of the actual degradation function that is possibly relatable to the inertial drivetrain properties of the considered wind turbine. However, further research is needed to substantiate the latter articulated claim.

5.3 Data batch size

As the learning scheme is based on steady-state assumptions, an extended data batch size is needed to average out dynamic effects from the collected data set. This section exposes the impact of varying the data set data batch size N and determines what batch size is sufficient to acquire decent learning performance. Fig. 5 shows the analysis results for the following set of batch sizes $N = (1/T_{\text{s}})\,\{50,\ 200,\ 1000\}$.

The results expose the foreseeable trend that the variance over the learned degradation profiles decreases for increased data batch sizes. A data set corresponding to or larger than a simulation length of $T_{\text{sim}} = 1000$ s seems sufficient to obtain consistent results.

6. CONCLUSIONS

This paper presents a novel excitation-free and data-driven learning algorithm to calibrate the model information in advanced wind turbine control schemes. The learning algorithm is based on steady-state assumptions, making its derivation concise for physical interpretation and straightforward in its implementation. The algorithm only relies upon closed-loop measurements of a wind turbine, augmented with an externally acquired rotor-effective wind speed measurement. The learning procedure is iterative because, after data collection under nominal closed-loop turbine operation, a correction factor is computed to update the control scheme's internal model. This procedure is repetitive until convergence at the current operating point. Under realistic turbulent wind conditions, the learning algorithm can calibrate the internal model to represent the actual aerodynamic turbine properties accurately. A sensitivity study exposes algorithm requirements on the measurement bandwidth of the REWS, shows the susceptibility to measurement offsets, and conditions on the data collection time.

REFERENCES

Abbas, N.J., Zalkind, D.S., Pao, L., and Wright, A. (2022). A reference open-source controller for fixed and floating offshore wind turbines. *Wind Energy Science*.

Bossanyi, E.A. (2000). The design of closed loop controllers for wind turbines. *Wind Energy*.

Brandetti, L., Liu, Y., Mulders, S.P., Ferreira, C., Watson, S., and van Wingerden, J.W. (2022). On the ill-conditioning of the combined wind speed estimator and tip-speed ratio tracking control scheme. *Journal of Physics: Conference Series*.

Burton, T., Jenkins, N., Sharpe, D., and Bossanyi, E.A. (2001). *Wind energy handbook*. John Wiley & Sons, Chichester, United Kingdom.

De Kooning, J.D.M., Gevaert, L., Van de Vyver, J., Vandoorn, T.L., and Vandevelde, L. (2013). Online estimation of the power coefficient versus tip-speed ratio curve of wind turbines. In *Industrial Electronics Society Conference (IECON)*.

Fingersh, L.J. and Carlin, P. (1999). Results from the NREL variable-speed test bed. In *Proc. 17th ASME Wind Energy Symp.*

Global Wind Energy Council (2022). Global Wind Report 2022. Technical report.

IEC (2019). IEC 61400-1: Wind turbines - Part 1: Design requirements. Report, International Electrotechnical Commission.

Johnson, K.E., Pao, L.Y., Balas, M.J., and Lee, J.F. (2006). Control variable-speed wind turbines: Standard and adaptive techniques for maximizing energy capture. *IEEE Control Systems*.

Johnson, K., Pao, L., Balas, M., Kulkami, V., and Fingersh, L. (2004). Stability analysis of an adaptive torque controller for variable speed wind turbines. In *Conference on Decision and Control (CDC)*.

Jonkman, J., Butterfield, S., Musial, W., and Scott, G. (2009). Definition of a 5-MW reference wind turbine for offshore system development. Technical report, National Renewable Energy Laboratory (NREL), Golden, Colorado.

Komusanac, I., Brindley, G., Fraile, D., and Ramirez, L. (2022). Wind Energy in Europe - 2021 Statistics and the outlook for 2022-2026. Technical report.

Lio, W.H., Li, A., and Meng, F. (2021). Real-time rotor effective wind speed estimation using Gaussian process regression and Kalman filtering. *Renewable Energy*.

Liu, Y., Pamososuryo, A.K., Ferrari, R.M., and van Wingerden, J.W. (2022). The Immersion and Invariance wind speed estimator revisited and new results. *IEEE Control Systems Letters*.

Mulders, S., Brandetti, L., Spagnolo, F., Liu, Y., Christensen, P., and van Wingerden, J.W. (2023a). A learning algorithm for the calibration of internal model uncertainties in advanced wind turbine controllers: A wind speed measurement-free approach. In *American Control Conference (ACC)*.

Mulders, S., Spagnolo, F., Liu, Y., Christensen, P., and van Wingerden, J. (2023b). Software implementation: A data-driven learning algorithm calibrating the internal model for advanced wind turbine controllers.

Ortega, R., Mancilla-David, F., and Jaramillo, F. (2013). A globally convergent wind speed estimator for wind turbine systems. *International Journal of Adaptive Control and Signal Processing*, 27.

Rotea, M.A. (2017). Logarithmic power feedback for extremum seeking control of wind turbines. In *20th IFAC World Congress*.

Soltani, M.N., Knudsen, T., Svenstrup, M., Wisniewski, R., Brath, P., Ortega, R., and Johnson, K. (2013). Estimation of rotor effective wind speed: A comparison. *IEEE Transactions on Control Systems Technology*.

Veers, P., Dykes, K., Lantz, E., Barth, S., Bottasso, C.L., Carlson, O., Clifton, A., Green, J., Green, P., Holttinen, H., Laird, D., Lehtomäki, V., Lundquist, J.K., Manwell, J., Marquis, M., Meneveau, C., Moriarty, P., Munduate, X., Muskulus, M., Naughton, J., Pao, L., Paquette, J., Peinke, J., Robertson, A., Rodrigo, J.S., Sempreviva, A.M., Smith, J.C., Tuohy, A., and Wiser, R. (2019). Grand challenges in the science of wind energy. *Science*.

Appendix A. ILL-CONDITIONING

This section provides further context on the introduced inequality and the related problem of ill-conditioning present in estimator-based wind turbine controllers, such as the WSE-TSR scheme considered in this paper. Equation (11) holds for the closed-loop controlled system in steady-state as the equality of the products

$$C_{\mathrm{P}}(\lambda)U^3 = \hat{C}_{\mathrm{P}}(\hat{\lambda})\hat{U}^3$$

is satisfied regardless of the level of uncertainty in the internal model. That is, biased power coefficient information to the actual aerodynamic characteristics is compensated for by a biased wind speed estimate. In this way, the equality of the power coefficient-wind speed always holds in steady state, whereas the actual and estimated representations of the individual terms might be dissimilar. This phenomenon has been extensively described and analyzed in (Brandetti et al., 2022) and is referred to as the problem of ill-conditioning.

Now, when an external measured signal replaces the wind-speed estimate resulting from the closed-loop observer-controller-based control scheme, the previously-described balancing mechanism is negated, resulting in the inequality of (12).